



Measurements of the masses and widths of the $\Sigma_c(2455)^{0/++}$ and $\Sigma_c(2520)^{0/++}$ baryons

S.-H. Lee,²⁸ B. R. Ko,²⁸ E. Won,²⁸ A. Abdesselam,⁵⁷ I. Adachi,¹³ H. Aihara,⁶³
D. M. Asner,⁴⁹ T. Aushev,²² R. Ayad,⁵⁷ A. M. Bakich,⁵⁶ A. Bala,⁵⁰ V. Bansal,⁴⁹
V. Bhardwaj,⁴⁰ B. Bhuyan,¹⁶ G. Bonvicini,⁶⁹ A. Bozek,⁴⁴ T. E. Browder,¹² D. Červenkov,⁴
A. Chen,⁴¹ B. G. Cheon,¹¹ R. Chistov,²² K. Cho,²⁷ V. Chobanova,³⁴ S.-K. Choi,¹⁰
Y. Choi,⁵⁵ D. Cinabro,⁶⁹ J. Dalseno,^{34,59} M. Danilov,^{22,36} Z. Doležal,⁴ Z. Drásal,⁴
A. Drutskey,^{22,36} S. Eidelman,³ D. Epifanov,⁶³ H. Farhat,⁶⁹ J. E. Fast,⁴⁹ T. Ferber,⁶
A. Frey,⁹ V. Gaur,⁵⁸ N. Gabyshev,³ S. Ganguly,⁶⁹ A. Garmash,³ R. Gillard,⁶⁹ Y. M. Goh,¹¹
B. Golob,^{31,23} H. Hayashii,⁴⁰ X. H. He,⁵¹ Y. Hoshi,⁶¹ H. J. Hyun,²⁹ T. Iijima,^{39,38}
A. Ishikawa,⁶² R. Itoh,¹³ Y. Iwasaki,¹³ T. Iwashita,²⁶ I. Jaegle,¹² T. Julius,³⁵ J. H. Kang,⁷¹
Y. Kato,³⁸ T. Kawasaki,⁴⁶ C. Kiesling,³⁴ B. H. Kim,⁵³ D. Y. Kim,⁵⁴ J. B. Kim,²⁸
J. H. Kim,²⁷ M. J. Kim,²⁹ K. Kinoshita,⁵ J. Klucar,²³ P. Kodyš,⁴ S. Korpar,^{33,23}
P. Križan,^{31,23} P. Krokovny,³ T. Kuhr,²⁵ T. Kumita,⁶⁵ Y.-J. Kwon,⁷¹ J. S. Lange,⁷
Y. Li,⁶⁸ L. Li Gioi,³⁴ J. Libby,¹⁷ D. Liventsev,¹³ D. Matvienko,³ K. Miyabayashi,⁴⁰
H. Miyata,⁴⁶ A. Moll,^{34,59} T. Mori,³⁸ R. Mussa,²¹ Y. Nagasaka,¹⁴ E. Nakano,⁴⁸ M. Nakao,¹³
M. Nayak,¹⁷ E. Nedelkovska,³⁴ N. K. Nisar,⁵⁸ S. Nishida,¹³ O. Nitoh,⁶⁶ S. Ogawa,⁶⁰
S. Okuno,²⁴ P. Pakhlov,^{22,36} G. Pakhlova,²² H. K. Park,²⁹ T. K. Pedlar,³² T. Peng,⁵²
R. Pestotnik,²³ M. Petrič,²³ L. E. Piilonen,⁶⁸ A. Poluektov,³ E. Ríbežl,²³ M. Ritter,³⁴
M. Röhrken,²⁵ A. Rostomyan,⁶ S. Ryu,⁵³ H. Sahoo,¹² T. Saito,⁶² K. Sakai,¹³ Y. Sakai,¹³
S. Sandilya,⁵⁸ D. Santel,⁵ L. Santelj,²³ T. Sanuki,⁶² Y. Sato,⁶² O. Schneider,³⁰
G. Schnell,^{1,15} C. Schwanda,¹⁹ D. Semmler,⁷ K. Senyo,⁷⁰ O. Seon,³⁸ M. E. Sevier,³⁵
M. Shapkin,²⁰ V. Shebalin,³ C. P. Shen,² T.-A. Shibata,⁶⁴ J.-G. Shiu,⁴³ A. Sibidanov,⁵⁶
Y.-S. Sohn,⁷¹ E. Solovieva,²² S. Stanič,⁴⁷ M. Starič,²³ M. Steder,⁶ M. Sumihama,⁸
T. Sumiyoshi,⁶⁵ U. Tamponi,^{21,67} K. Tanida,⁵³ Y. Teramoto,⁴⁸ K. Trabelsi,¹³
M. Uchida,⁶⁴ S. Uehara,¹³ T. Uglov,^{22,37} S. Uno,¹³ C. Van Hulse,¹ P. Vanhoefer,³⁴
G. Varner,¹² K. E. Varvell,⁵⁶ A. Vinokurova,³ M. N. Wagner,⁷ C. H. Wang,⁴²
P. Wang,¹⁸ M. Watanabe,⁴⁶ Y. Watanabe,²⁴ K. M. Williams,⁶⁸ Y. Yamashita,⁴⁵
S. Yashchenko,⁶ Y. Yook,⁷¹ C. Z. Yuan,¹⁸ V. Zhilich,³ V. Zhulanov,³ and A. Zupanc²³

(The Belle Collaboration)

¹University of the Basque Country UPV/EHU, 48080 Bilbao

²Beihang University, Beijing 100191

³Budker Institute of Nuclear Physics SB RAS and
Novosibirsk State University, Novosibirsk 630090

⁴Faculty of Mathematics and Physics, Charles University, 121 16 Prague

- ⁵University of Cincinnati, Cincinnati, Ohio 45221
⁶Deutsches Elektronen-Synchrotron, 22607 Hamburg
⁷Justus-Liebig-Universität Gießen, 35392 Gießen
⁸Gifu University, Gifu 501-1193
⁹II. Physikalisches Institut, Georg-August-Universität Göttingen, 37073 Göttingen
¹⁰Gyeongsang National University, Chinju 660-701
¹¹Hanyang University, Seoul 133-791
¹²University of Hawaii, Honolulu, Hawaii 96822
¹³High Energy Accelerator Research Organization (KEK), Tsukuba 305-0801
¹⁴Hiroshima Institute of Technology, Hiroshima 731-5193
¹⁵IKERBASQUE, Basque Foundation for Science, 48011 Bilbao
¹⁶Indian Institute of Technology Guwahati, Assam 781039
¹⁷Indian Institute of Technology Madras, Chennai 600036
¹⁸Institute of High Energy Physics,
Chinese Academy of Sciences, Beijing 100049
¹⁹Institute of High Energy Physics, Vienna 1050
²⁰Institute for High Energy Physics, Protvino 142281
²¹INFN - Sezione di Torino, 10125 Torino
²²Institute for Theoretical and Experimental Physics, Moscow 117218
²³J. Stefan Institute, 1000 Ljubljana
²⁴Kanagawa University, Yokohama 221-8686
²⁵Institut für Experimentelle Kernphysik,
Karlsruher Institut für Technologie, 76131 Karlsruhe
²⁶Kavli Institute for the Physics and Mathematics of the Universe (WPI),
University of Tokyo, Kashiwa 277-8583
²⁷Korea Institute of Science and Technology Information, Daejeon 305-806
²⁸Korea University, Seoul 136-713
²⁹Kyungpook National University, Daegu 702-701
³⁰École Polytechnique Fédérale de Lausanne (EPFL), Lausanne 1015
³¹Faculty of Mathematics and Physics,
University of Ljubljana, 1000 Ljubljana
³²Luther College, Decorah, Iowa 52101
³³University of Maribor, 2000 Maribor
³⁴Max-Planck-Institut für Physik, 80805 München
³⁵School of Physics, University of Melbourne, Victoria 3010
³⁶Moscow Physical Engineering Institute, Moscow 115409
³⁷Moscow Institute of Physics and Technology, Moscow Region 141700
³⁸Graduate School of Science, Nagoya University, Nagoya 464-8602
³⁹Kobayashi-Maskawa Institute, Nagoya University, Nagoya 464-8602
⁴⁰Nara Women's University, Nara 630-8506
⁴¹National Central University, Chung-li 32054
⁴²National United University, Miao Li 36003
⁴³Department of Physics, National Taiwan University, Taipei 10617
⁴⁴H. Niewodniczanski Institute of Nuclear Physics, Krakow 31-342
⁴⁵Nippon Dental University, Niigata 951-8580
⁴⁶Niigata University, Niigata 950-2181
⁴⁷University of Nova Gorica, 5000 Nova Gorica

- ⁴⁸*Osaka City University, Osaka 558-8585*
- ⁴⁹*Pacific Northwest National Laboratory, Richland, Washington 99352*
- ⁵⁰*Panjab University, Chandigarh 160014*
- ⁵¹*Peking University, Beijing 100871*
- ⁵²*University of Science and Technology of China, Hefei 230026*
- ⁵³*Seoul National University, Seoul 151-742*
- ⁵⁴*Soongsil University, Seoul 156-743*
- ⁵⁵*Sungkyunkwan University, Suwon 440-746*
- ⁵⁶*School of Physics, University of Sydney, NSW 2006*
- ⁵⁷*Department of Physics, Faculty of Science, University of Tabuk, Tabuk 71451*
- ⁵⁸*Tata Institute of Fundamental Research, Mumbai 400005*
- ⁵⁹*Excellence Cluster Universe, Technische Universität München, 85748 Garching*
- ⁶⁰*Toho University, Funabashi 274-8510*
- ⁶¹*Tohoku Gakuin University, Tagajo 985-8537*
- ⁶²*Tohoku University, Sendai 980-8578*
- ⁶³*Department of Physics, University of Tokyo, Tokyo 113-0033*
- ⁶⁴*Tokyo Institute of Technology, Tokyo 152-8550*
- ⁶⁵*Tokyo Metropolitan University, Tokyo 192-0397*
- ⁶⁶*Tokyo University of Agriculture and Technology, Tokyo 184-8588*
- ⁶⁷*University of Torino, 10124 Torino*
- ⁶⁸*CNP, Virginia Polytechnic Institute and State University, Blacksburg, Virginia 24061*
- ⁶⁹*Wayne State University, Detroit, Michigan 48202*
- ⁷⁰*Yamagata University, Yamagata 990-8560*
- ⁷¹*Yonsei University, Seoul 120-749*

Abstract

We present measurements of the masses and decay widths of the baryonic states $\Sigma_c(2455)^{0/++}$ and $\Sigma_c(2520)^{0/++}$ using a data sample corresponding to an integrated luminosity of 711 fb^{-1} collected with the Belle detector at the KEKB e^+e^- asymmetric-energy collider operating at the $\Upsilon(4S)$ resonance. We report the mass differences with respect to the Λ_c^+ baryon

$$\begin{aligned} M(\Sigma_c(2455)^0) - M(\Lambda_c^+) &= 167.29 \pm 0.01 \pm 0.02 \text{ MeV}/c^2, \\ M(\Sigma_c(2455)^{++}) - M(\Lambda_c^+) &= 167.51 \pm 0.01 \pm 0.02 \text{ MeV}/c^2, \\ M(\Sigma_c(2520)^0) - M(\Lambda_c^+) &= 231.98 \pm 0.11 \pm 0.04 \text{ MeV}/c^2, \\ M(\Sigma_c(2520)^{++}) - M(\Lambda_c^+) &= 231.99 \pm 0.10 \pm 0.02 \text{ MeV}/c^2, \end{aligned}$$

and the decay widths

$$\begin{aligned} \Gamma(\Sigma_c(2455)^0) &= 1.76 \pm 0.04_{-0.21}^{+0.09} \text{ MeV}/c^2, \\ \Gamma(\Sigma_c(2455)^{++}) &= 1.84 \pm 0.04_{-0.20}^{+0.07} \text{ MeV}/c^2, \\ \Gamma(\Sigma_c(2520)^0) &= 15.41 \pm 0.41_{-0.32}^{+0.20} \text{ MeV}/c^2, \\ \Gamma(\Sigma_c(2520)^{++}) &= 14.77 \pm 0.25_{-0.30}^{+0.18} \text{ MeV}/c^2, \end{aligned}$$

where the first uncertainties are statistical and the second are systematic. The isospin mass splittings are measured to be $M(\Sigma_c(2455)^{++}) - M(\Sigma_c(2455)^0) = 0.22 \pm 0.01 \pm 0.01 \text{ MeV}/c^2$ and $M(\Sigma_c(2520)^{++}) - M(\Sigma_c(2520)^0) = 0.01 \pm 0.15 \pm 0.03 \text{ MeV}/c^2$. These results are the most precise to date.

PACS numbers: 14.20.Lq, 14.20.-c, 14.20.Gk

I. INTRODUCTION

Properties of heavy-flavored hadrons such as masses and decay widths can, in principle, be described in the theoretical framework of quantum chromodynamics (QCD). However, they are difficult to calculate in practice with the perturbative QCD technique due to the fact that the strong coupling constant α_s is large in this low energy regime. To overcome this difficulty, other methods such as lattice QCD [1–3], heavy quark effective theory [4], quark model [5], QCD sum rule [6], and bag model [7] are deployed.

The properties of the $\Sigma_c^{0/++}$ baryons have been measured by many experiments [8–14], but the total uncertainties of the world averages remain large [15]. For example, the relative uncertainties of the decay widths are around 10% of their central values. Furthermore, the relative uncertainty of the mass splitting $m(\Sigma_c(2455)^{++}) - m(\Sigma_c(2455)^0)$ is about 40%, and there is no significant measurement for the mass splitting $m(\Sigma_c(2520)^{++}) - m(\Sigma_c(2520)^0)$ [12, 16]. Due to the mass hierarchy between the d and u quarks, one may expect that the Σ_c^0 (ddc) baryon is heavier than the Σ_c^{++} (uuc) baryon; however, many experimental results contradict this naive expectation [8, 11–13]. To explain the discrepancy, various models have been introduced [17–23] that predict positive mass splittings. Precise measurements of the mass splittings are necessary to test these models.

In this paper, we present precise measurements of the masses and decay widths of the $\Sigma_c(2455)^{0/++}$ and $\Sigma_c(2520)^{0/++}$ baryons, and of their mass splittings. Throughout this paper, the charge-conjugate decay modes are implied.

II. DATA SAMPLES AND EVENT SELECTIONS

This study uses a data sample corresponding to an integrated luminosity of 711 fb^{-1} collected with the Belle detector at the KEKB e^+e^- asymmetric-energy collider [24] operating at the $\Upsilon(4S)$ resonance. The Belle detector is a large solid angle magnetic spectrometer that consists of a silicon vertex detector (SVD), a 50-layer central drift chamber (CDC), an array of aerogel threshold Cherenkov counters (ACC), a barrel-like arrangement of time-of-flight scintillation counters (TOF), and an electromagnetic calorimeter comprising CsI(Tl) crystals located inside a superconducting solenoid coil that provides a 1.5 T magnetic field. An iron flux return located outside the coil is instrumented to detect K_L^0 mesons and to identify muons. A detailed description of the Belle detector can be found in Ref. [25].

The $\Sigma_c^{0/++}$ baryons are reconstructed via their $\Sigma_c^{0/++} \rightarrow \Lambda_c^+(\rightarrow pK^-\pi^+)\pi_s^{-/+}$ decays, where π_s is a low-momentum (“slow”) pion. Charged tracks are required to have an impact parameter with respect to the interaction point of less than 3 cm along the beam direction (the z axis) and less than 1 cm in the plane transverse to the beam direction. In addition, each track is required to have at least two associated vertex detector hits each in the z and azimuthal strips of the SVD. The particles are identified using likelihood [26] criteria that have efficiencies of 84%, 91%, 93%, and 99% for p , K , π , and π_s , respectively. Λ_c^+ candidates are reconstructed as combinations of p , K^- , and π^+ candidates with an invariant mass between 2278.07 and 2295.27 MeV/c^2 , corresponding to $\pm 2.1\sigma$ around the nominal Λ_c^+ mass, where σ represents the Λ_c^+ invariant mass resolution. Λ_c^+ daughter tracks are refit assuming they originate from a common vertex. The Λ_c^+ production vertex is defined by the intersection of its trajectory with the e^+e^- interaction region. Λ_c^+ candidates are combined with π_s candidates to form $\Sigma_c^{0/++}$ candidates. π_s candidates are required to

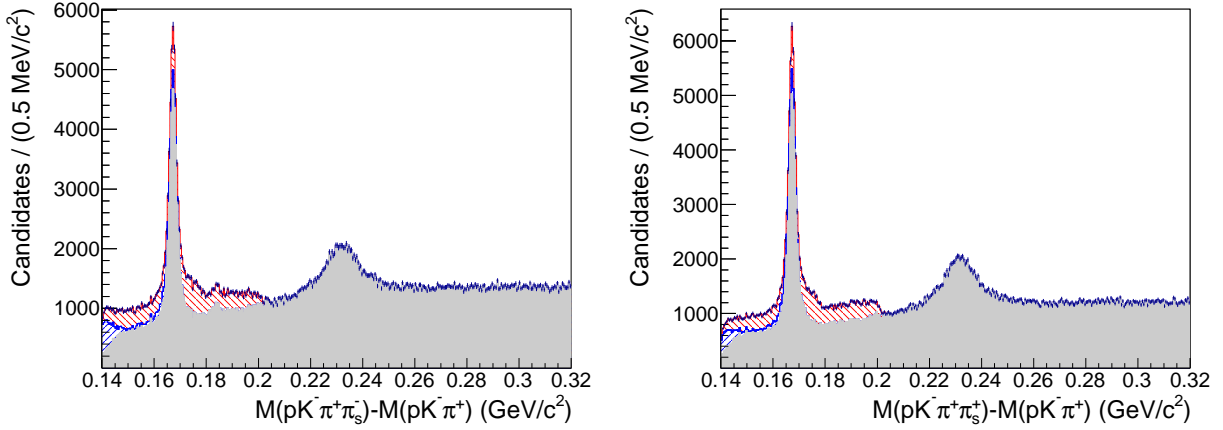


FIG. 1: $M(pK^-\pi^+\pi_s^-) - M(pK^-\pi^+)$ (left) and $M(pK^-\pi^+\pi_s^+) - M(pK^-\pi^+)$ (right) distributions before (points) and after (shaded) the feed-down subtraction. The subtracted feed-down backgrounds from the $\Lambda_c(2595)^+$ (left-hatched) and $\Lambda_c(2625)^+$ (right-hatched) are also shown. The first and second peaks correspond to the $\Sigma_c(2455)^{0/++}$ and $\Sigma_c(2520)^{0/++}$ signals.

originate from the Λ_c^+ production vertex in order to improve their momentum resolution, which results in an enhanced signal-to-background ratio. Signal candidates retained for further analysis are required to have a confidence level greater than 0.1% for the π_s vertex fit constrained to the Λ_c^+ production vertex. To suppress combinatorial backgrounds, we also require the momentum of $\Sigma_c^{0/++}$ baryons in the center-of-mass frame to be greater than 2.0 GeV/c. The distributions of the mass difference $\Delta M \equiv M(pK^-\pi^+\pi_s^{-/+}) - M(pK^-\pi^+)$ for all reconstructed $\Sigma_c^{0/++}$ candidates are shown in Fig. 1.

We also use a Monte Carlo (MC) simulation sample for various purposes in this study, where events are generated with PYTHIA [27], decays of unstable particles are modeled with EVTGEN [28], and the detector response is simulated with GEANT3 [29].

III. BACKGROUNDS

The sample of selected $\Sigma_c^{0/++}$ candidates includes two types of backgrounds: partially reconstructed decays of excited Λ_c^+ baryons (referred to as “feed-down backgrounds”) and random combinations of the final state particles. The procedures used to parameterize these backgrounds are described in this section.

A. Feed-down backgrounds from excited Λ_c^+ baryons

From the tracks of a $\Lambda_c^{*+} \rightarrow \Lambda_c^+ \pi_s^+ \pi_s^-$ decay, a Σ_c candidate can be reconstructed if one of the slow pions is left out. This can be either a signal (from a $\Sigma_c^{0/++}$ resonant decay of an excited Λ_c^+ state) or a feed-down background event. The feed-down backgrounds from the $\Lambda_c(2595)^+$ and $\Lambda_c(2625)^+$ states appear in the $\Sigma_c(2455)^{0/++}$ mass region. In order to remove these backgrounds, we tag events that have a mass difference $M(pK^-\pi^+\pi_s^{-/+}h^{+/-}) - M(pK^-\pi^+)$ ($h^{+/-}$ being a charged track) that falls either in the [302, 312] MeV/c² or the [336, 347] MeV/c² mass interval, corresponding to the $\Lambda_c(2595)^+$ and $\Lambda_c(2625)^+$ signals,

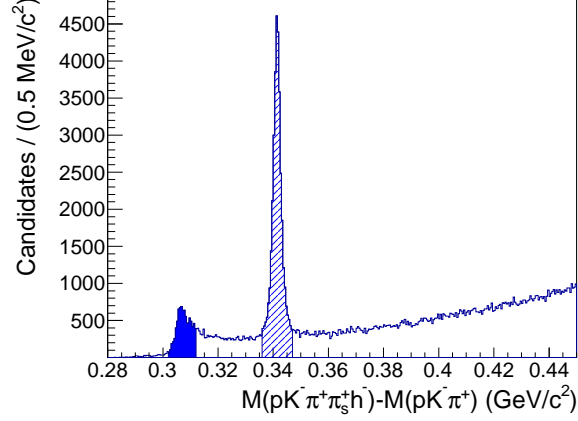


FIG. 2: Mass difference of $M(pK^-\pi^+\pi_s^+h^-) - M(pK^-\pi^+)$. Signal regions of the $\Lambda_c(2595)^+$ (filled) and $\Lambda_c(2625)^+$ (hatched) are defined in the text.

respectively (see Fig. 2). The tagged events are subtracted from the ΔM distributions as shown in Fig. 1. To prevent a possible bias in the subtraction, we estimate the backgrounds under the Λ_c^{*+} peaks from MC simulations and subtract them from the tagged feed-down backgrounds. Furthermore, we take into account the charged track detection efficiency of 74% on average to correct for the feed-down backgrounds. Since the shape of the feed-down backgrounds depends on the π_s momentum, we obtain and apply the efficiency correction as a function of this quantity.

B. Random backgrounds

The remaining background consists of random combinations, with or without a true Λ_c^+ baryon. In the latter case, the background level is estimated from the Λ_c^+ mass sidebands, defined as $M(pK^-\pi^+) \in [2259.16, 2267.76] \text{ MeV}/c^2$ or $M(pK^-\pi^+) \in [2305.58, 2314.18] \text{ MeV}/c^2$. The treatment of the random backgrounds in the fit is discussed in Sec. IV.

IV. FIT PROCEDURE

The parameters of the $\Sigma_c(2455)^{0/++}$ and $\Sigma_c(2520)^{0/++}$ signals, namely the decay widths and the mass differences with respect to the Λ_c^+ mass, are determined by performing binned maximum likelihood fits. Due to the small fraction of the weighted events in the region where the feed-down background is subtracted, a correction to the covariance matrix of the fit parameters is applied to obtain the proper errors. The $\Sigma_c(2455)^{0/++}$ and $\Sigma_c(2520)^{0/++}$ baryons are described by a relativistic Breit-Wigner probability density function (PDF) convolved with the detector response function as

$$\int_{-\infty}^{+\infty} T(\Delta M'; \Delta M_0, \Gamma) R(\Delta M - \Delta M') d(\Delta M')$$

where $T(\Delta M; \Delta M_0, \Gamma)$ is a relativistic Breit-Wigner with the nominal mass difference $\Delta M_0 \equiv M(\Sigma_c) - M(\Lambda_c^+)$ and the decay width Γ as fit parameters, and R is the detector response function.

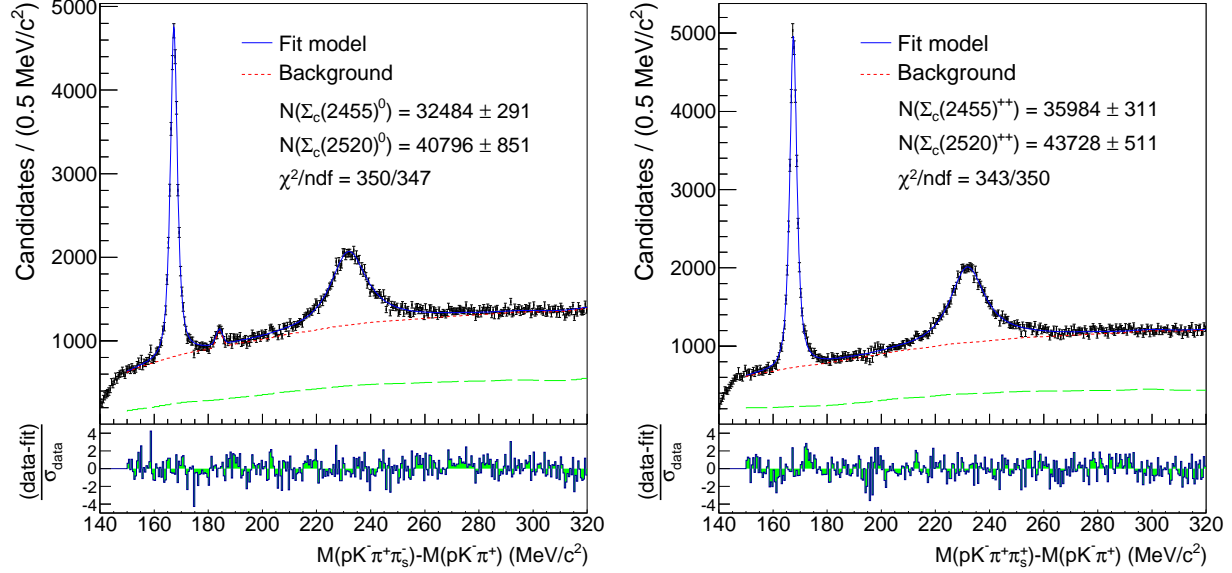


FIG. 3: Fits to the mass differences $M(pK^- \pi^+ \pi_s^-) - M(pK^- \pi^+)$ (left) and $M(pK^- \pi^+ \pi_s^+) - M(pK^- \pi^+)$ (right) obtained from data (points with error bar) with the models (solid lines) described in the text. The random backgrounds without true Λ_c^+ baryons (long-dashed line) and the total backgrounds (dashed lines) are shown as well. The peak near 185 MeV/c² in the left plot is due to the $\Xi_c^0 \rightarrow \Lambda_c^+ \pi^-$ decay. The fit signal yields as well as the fit χ^2 per degree of freedom are indicated on the plots. The bottom histograms are the differences between the values of data and fit divided by the statistical uncertainties of data to illustrate the fit quality.

The resolution function R is parameterized as the sum of three Gaussian functions centered at zero. The parameters are obtained from an MC simulation separately for the $\Sigma_c(2455)$ and $\Sigma_c(2520)$ signals. The detector resolutions for the $\Sigma_c(2455)$ and $\Sigma_c(2520)$ baryons are found to be 1.012 ± 0.001 and 1.578 ± 0.013 MeV/c², respectively, from the weighted variances of the three Gaussian distributions where the errors are statistical.

The random backgrounds without true Λ_c^+ baryons are modeled as histogram PDFs with shape and normalization taken from the Λ_c^+ baryon data sidebands. The random backgrounds with true Λ_c^+ baryons are described with a threshold function:

$$(\Delta M - m_\pi)^{c_0} e^{c_1(\Delta M - m_\pi)},$$

where c_0 , c_1 are fit parameters and m_π is the known charged pion mass [15].

In the neutral channel, we find a small peak near $\Delta M = 185$ MeV/c². Based on studies performed using MC and data samples, we confirm the origin of this peak to be the as-of-yet unobserved decay of $\Xi_c^0 \rightarrow \Lambda_c^+ \pi^-$. We describe this peak with a Gaussian function. The mean and width of the Gaussian from the fit are found to be 184.08 ± 0.15 and 1.21 ± 0.17 MeV/c², respectively; the former is consistent with that from the world average ($m(\Xi_c^0) - m(\Lambda_c^+) = 184.42_{-0.81}^{+0.37}$ MeV/c²) [15] and the latter is consistent with that from MC.

The fit results to ΔM are shown in Fig. 3. The goodness-of-fit values are $\chi^2 = 350$ with 347 degrees of freedom for Σ_c^0 and $\chi^2 = 343$ with 350 degrees of freedom for Σ_c^{++} .

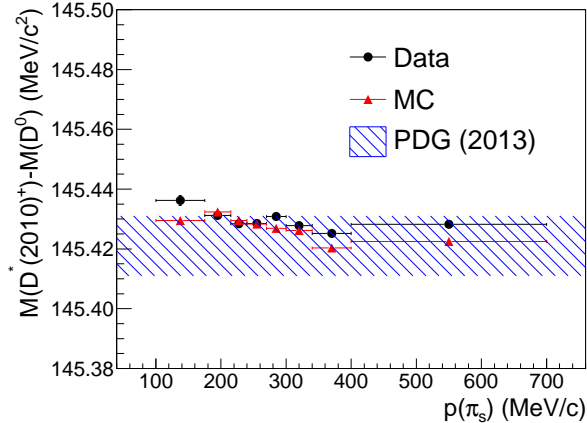


FIG. 4: Mass difference $M(D^*(2010)^+) - M(D^0)$ obtained from MC (red triangle) and data (black circle) using the $D^*(2010)^+ \rightarrow D^0(\rightarrow K^-\pi^+)\pi_s^+$ decay as a function of the π_s momentum. The uncertainties of each points are too small to be displayed. The world average with its total uncertainty [15] is also shown as a hatched area.

V. SYSTEMATIC UNCERTAINTIES

To estimate systematic uncertainties, three sources are studied: momentum scale, resolution and fit model, and background parameterization. These are summarized in Table I.

A. Momentum calibration

Mass measurements are sensitive to the momentum scale of the detector. Because there is a possible bias in the measurements of the charged track momenta, which may be due to the energy loss of the charged particles in materials, one should consider the precision of the momentum calibration. To minimize the possible bias, we calibrate the momentum scale using the copious $K_S^0 \rightarrow \pi^+\pi^-$ sample. Charged tracks are iteratively calibrated as functions of the curvature, polar angle, and momentum of each track in the laboratory frame by comparing the reconstructed and world average [15] masses of K_S^0 meson as a function of the K_S^0 momentum. The obtained corrections are applied to the data sets used in this study. To estimate the accuracy, we choose a control sample of $D^*(2010)^+ \rightarrow D^0(\rightarrow K^-\pi^+)\pi_s^+$ decay, and compare the mass difference of $M(D^*(2010)^+) - M(D^0)$ over the π_s momentum bins with the world average [15] as shown in Fig. 4. We observe the largest difference to be $0.02 \text{ MeV}/c^2$, which we assign as the systematic uncertainty on the mass difference measurements due to the momentum calibration.

B. Resolution model

Since our detector resolution model is evaluated from the MC as discussed in Sec. IV, the discrepancy between the MC and data is considered as a source of systematic uncertainty. To estimate the discrepancy, we compare the detector resolution in data and MC using the same control sample of $D^*(2010)^+ \rightarrow D^0(\rightarrow K^-\pi^+)\pi_s^+$ decay. Since the decay width of

the $D^*(2010)^+$ meson is small, one can assume that the distribution of the mass difference $M(D^*(2010)^+) - M(D^0)$ is dominated by the detector resolution. We vary the widths of the detector response functions from +1.7% to +11.8% in the fits to ΔM by choosing the largest and smallest differences between the MC and data obtained by comparing $M(D^*(2010)^+) - M(D^0)$ as a function of the π_s momentum. The uncertainties are found to be 0.19, 0.25, and 0.24 MeV/ c^2 for the widths of the $\Sigma_c(2455)^{0/++}$, $\Sigma_c(2520)^0$, and $\Sigma_c(2520)^{++}$ baryons, respectively. We also vary the detector response functions by $\pm 1\sigma$ deviation from the fitted resolution parameters, where σ is the statistical error, and only small uncertainties are found for the decay widths of 0.01 and 0.04 MeV/ c^2 for the $\Sigma_c(2455)^{0/++}$ and $\Sigma_c(2520)^{0/++}$ baryons, respectively.

C. Fit model

We also check the internal consistency of the fitting procedure. In order to probe any bias from the fitter, we perform 10,000 pseudo-experiments for each of the mass differences, $\Delta M_0(\Sigma_c(2455))$ and $\Delta M_0(\Sigma_c(2520))$, and the decay widths $\Gamma(\Sigma_c(2455))$ and $\Gamma(\Sigma_c(2520))$. In the production of the pseudo-experiments, we set the input values to be those obtained from the data. From the study, we find negligible discrepancies.

The effect of binning is studied by varying the bin size in the fits to ΔM from 0.1 MeV/ c^2 to 1.0 MeV/ c^2 . The uncertainties of ΔM_0 are negligible, and we find small uncertainties for the widths of 0.09, 0.06, 0.04, and 0.05 MeV/ c^2 for the $\Sigma_c(2455)^0$, $\Sigma_c(2455)^{++}$, $\Sigma_c(2520)^0$, and the $\Sigma_c(2520)^{++}$ baryons, respectively.

We also test the effect of various fit ranges. We choose several fit ranges, some of which include both the $\Sigma_c(2455)^{0/++}$ and $\Sigma_c(2520)^{0/++}$ signals and others only one of them. Though the results from the various fit ranges are consistent within the statistical fluctuations, we conservatively assign the variations in the fit results, 0.03 and 0.01 MeV/ c^2 for $\Delta M_0(\Sigma_c(2520)^0)$ and $\Delta M_0(\Sigma_c(2520)^{++})$, respectively, and 0.19 and 0.17 MeV/ c^2 for the widths of the $\Sigma_c(2520)^0$ and $\Sigma_c(2520)^{++}$ baryons, respectively, as systematic uncertainties.

D. Background model

Since we correct the feed-down backgrounds by taking into account the efficiency as discussed in Sec. III, the uncertainty of the efficiency should also be taken into account. The systematic uncertainty from the feed-down model is estimated as 1.87% from the error propagation of the statistical uncertainties of the feed-down backgrounds, the uncertainties of the tracking efficiency and the acceptance of the detector. We vary the yields of the feed-down background by $\pm 1.87\%$ without significant effect on the fit results compared with the statistical uncertainties. Since we fix the yields of the random backgrounds without true Λ_c^+ baryons, as discussed in Sec. III, we also vary the yields of the random backgrounds by their uncertainties; only negligible effects are obtained. Finally, we test other threshold functions to describe the random backgrounds with true Λ_c^+ baryons, but again find only negligible effects.

TABLE I: Systematic uncertainties for the mass differences (ΔM_0) and the decay widths (Γ) of the $\Sigma_c(2455)^{0/++}$ and $\Sigma_c(2520)^{0/++}$ baryons in MeV/c^2 . The uncertainties for ΔM_0 from the resolution model and for Γ from the momentum calibration are insignificant.

	$\Sigma_c(2455)^0$		$\Sigma_c(2520)^0$		$\Sigma_c(2455)^{++}$		$\Sigma_c(2520)^{++}$	
	ΔM_0	Γ	ΔM_0	Γ	ΔM_0	Γ	ΔM_0	Γ
Momentum calibration	± 0.02	—	± 0.02	—	± 0.02	—	± 0.02	—
Resolution model	—	$^{+0.01}_{-0.19}$	—	$^{+0.04}_{-0.25}$	—	$^{+0.01}_{-0.19}$	—	$^{+0.04}_{-0.24}$
Fit model	± 0.01	± 0.09	± 0.03	± 0.20	± 0.01	± 0.07	± 0.01	± 0.18
Total	± 0.02	$^{+0.09}_{-0.21}$	± 0.04	$^{+0.20}_{-0.32}$	± 0.02	$^{+0.07}_{-0.20}$	± 0.02	$^{+0.18}_{-0.30}$

TABLE II: The measurements of the masses (M_0) and the widths (Γ) of the $\Sigma_c(2455)^{0/++}$ and $\Sigma_c(2520)^{0/++}$ baryons. The first error is statistical and the second is systematic. The masses are calculated by adding the world average of Λ_c^+ mass to the mass differences (ΔM_0) and the third error is the total uncertainty of the world average of Λ_c^+ mass [15].

	ΔM_0 (MeV/c^2)	Γ (MeV/c^2)	M_0 (MeV/c^2)
$\Sigma_c(2455)^0$	$167.29 \pm 0.01 \pm 0.02$	$1.76 \pm 0.04^{+0.09}_{-0.21}$	$2453.75 \pm 0.01 \pm 0.02 \pm 0.14$
$\Sigma_c(2455)^{++}$	$167.51 \pm 0.01 \pm 0.02$	$1.84 \pm 0.04^{+0.07}_{-0.20}$	$2453.97 \pm 0.01 \pm 0.02 \pm 0.14$
$\Sigma_c(2520)^0$	$231.98 \pm 0.11 \pm 0.04$	$15.41 \pm 0.41^{+0.20}_{-0.32}$	$2518.44 \pm 0.11 \pm 0.04 \pm 0.14$
$\Sigma_c(2520)^{++}$	$231.99 \pm 0.10 \pm 0.02$	$14.77 \pm 0.25^{+0.18}_{-0.30}$	$2518.45 \pm 0.10 \pm 0.02 \pm 0.14$

VI. RESULTS

Our measurements for the mass differences (with respect to the Λ_c^+ mass) and the decay widths of the $\Sigma_c(2455)^{0/++}$ and $\Sigma_c(2520)^{0/++}$ baryons are summarized in Table II. We also calculate the mass splittings $M_0(\Sigma_c^{++}) - M_0(\Sigma_c^0)$ from $\Delta M_0(\Sigma_c^0)$ and $\Delta M_0(\Sigma_c^{++})$ as $M_0(\Sigma_c(2455)^{++}) - M_0(\Sigma_c(2455)^0) = 0.22 \pm 0.01 \pm 0.01 \text{ MeV}/c^2$ and $M_0(\Sigma_c(2520)^{++}) - M_0(\Sigma_c(2520)^0) = 0.01 \pm 0.15 \pm 0.03 \text{ MeV}/c^2$ where the first error is statistical and the second is systematic. Since the mass splittings are calculated from ΔM_0 , most of the systematic uncertainties cancel, such as that from the momentum calibration. These measurements are the most precise to date. The mass splitting $M_0(\Sigma_c(2455)^{++}) - M_0(\Sigma_c(2455)^0)$ is found to be positive as expected by the models [17–23].

Acknowledgments

We thank the KEKB group for the excellent operation of the accelerator; the KEK cryogenics group for the efficient operation of the solenoid; and the KEK computer group, the National Institute of Informatics, and the PNNL/EMSL computing group for valuable computing and SINET4 network support. We acknowledge support from the Ministry of Education, Culture, Sports, Science, and Technology (MEXT) of Japan, the Japan Society for the Promotion of Science (JSPS), and the Tau-Lepton Physics Research Center of Nagoya University; the Australian Research Council and the Australian Department of Industry, Innovation, Science and Research; Austrian Science Fund under Grant No. P 22742-N16; the National Natural Science Foundation of China under Contracts No. 10575109,

No. 10775142, No. 10825524, No. 10875115, No. 10935008 and No. 11175187; the Ministry of Education, Youth and Sports of the Czech Republic under Contract No. LG14034; the Carl Zeiss Foundation, the Deutsche Forschungsgemeinschaft and the Volkswagen-Stiftung; the Department of Science and Technology of India; the Istituto Nazionale di Fisica Nucleare of Italy; the WCU program of the Ministry Education Science and Technology, National Research Foundation of Korea Grants No. 2011-0029457, No. 2012-0008143, No. 2012R1A1A2008330, No. 2013R1A1A3007772; the BRL program under NRF Grant No. KRF-2011-0020333, No. KRF-2011-0021196, Center for Korean J-PARC Users, No. NRF-2013K1A3A7A06056592; the BK21 Plus program and the GSDC of the Korea Institute of Science and Technology Information; the Polish Ministry of Science and Higher Education and the National Science Center; the Ministry of Education and Science of the Russian Federation and the Russian Federal Agency for Atomic Energy; the Slovenian Research Agency; the Basque Foundation for Science (IKERBASQUE) and the UPV/EHU under program UFI 11/55; the Swiss National Science Foundation; the National Science Council and the Ministry of Education of Taiwan; and the U.S. Department of Energy and the National Science Foundation. This work is supported by a Grant-in-Aid from MEXT for Science Research in a Priority Area (“New Development of Flavor Physics”) and from JSPS for Creative Scientific Research (“Evolution of Tau-lepton Physics”). E. Won acknowledges support by NRF Grant No. 2010-0021174, B. R. Ko by NRF grant No. 2010-0021279.

-
- [1] R. Lewis, N. Mathur, and R. M. Woloshyn, Phys. Rev. D **64**, 094509 (2001).
 - [2] N. Mathur, R. Lewis, and R. M. Woloshyn, Phys. Rev. D **66**, 014502 (2002).
 - [3] Y. Namekawa *et al.*, Phys. Rev. D **87**, 094512 (2013).
 - [4] W. Roberts and M. Pervin, Int. J. Mod. Phys. A **23**, 2817 (2008).
 - [5] D. Ebert, R. N. Faustov, and V. O. Galkin, Phys. Lett. B **659**, 612 (2008).
 - [6] J. -R. Zhang and M. -Q. Huang, Phys. Rev. D **78**, 094015 (2008).
 - [7] A. Bernotas and V. Šimonis, Lith. J. Phys. **49**, 19 (2009).
 - [8] E. M. Aitala *et al.* (E791 collaboration), Phys. Lett. B **379**, 292 (1996).
 - [9] J. M. Link *et al.* (FOCUS collaboration), Phys. Lett. B **488**, 218 (2002).
 - [10] J. M. Link *et al.* (FOCUS collaboration), Phys. Lett. B **525**, 205 (2002).
 - [11] M. Artuso *et al.* (CLEO collaboration), Phys. Rev. D **65**, 071101(R) (2002).
 - [12] S. B. Athar *et al.* (CLEO collaboration), Phys. Rev. D **71**, 051101(R) (2005).
 - [13] T. Aaltonen *et al.* (CDF collaboration), Phys. Rev. D **84**, 012003 (2011).
 - [14] B. Aubert *et al.* (BaBar collaboration), Phys. Rev. D **78**, 112003 (2008).
 - [15] J. Beringer *et al.* (Particle Data Group), Phys. Rev. D **86**, 010001 (2012).
 - [16] G. Brandenburg *et al.* (CLEO collaboration), Phys. Rev. Lett. **78**, 2304 (1997).
 - [17] L. -H. Chan, Phys. Rev. D **31**, 204 (1985).
 - [18] W-Y. P. Hwang and D. B. Lichtenberg, Phys. Rev. D **35**, 3526 (1987).
 - [19] S. Capstick, Phys. Rev. D **36**, 2800 (1987).
 - [20] R. C. Verma and S. Srivastava, Phys. Rev. D **38**, 1623 (1988).
 - [21] R. E. Cutkosky and P. Geiger, Phys. Rev. D **48**, 1315 (1993).
 - [22] M. Genovese, J.-M. Richard, and B. Silvestre-Brac, Phys. Rev. D **59**, 014012 (1998).
 - [23] B. Silvestre-Brac, F. Brau, and C. Semay, J. Phys. G **29**, 2685 (2003).
 - [24] S. Kurokawa and E. Kikutani, Nucl. Instrum. Methods Phys. Res. Sect. A **499**, 1 (2003), and

- other papers included in this Volume; T.Abe *et al.*, Prog. Theor. Exp. Phys. **2013**, 03A001 (2013) and following articles up to 03A011.
- [25] A. Abashian *et al.* (Belle Collaboration), Nucl. Instrum. Methods Phys. Res. Sect. A **479**, 117 (2002); also see detector section in J. Brodzicka *et al.*, Prog. Theor. Exp. Phys. **2012**, 04D001 (2012).
 - [26] E. Nakano, Nucl. Instrum. Methods Phys. Res. Sect. A **494**, 402 (2002).
 - [27] T. Sjöstrand *et al.*, Comput. Phys. Commun. **135**, 238 (2001).
 - [28] D. J. Lange, Nucl. Instrum. Methods Phys. Res. Sect. A **462**, 152 (2001).
 - [29] R. Brun *et al.*, CERN Report DD/EE/84-1.